Design and Development of an Affordable Anthropomorphic Hand Prosthesis

Murilo C. Bicho
Centro de Ciências Computacionais
Universidade Federal do Rio Grande
Rio Grande, Brazil
0009-0007-3867-5387

Kristofer S. Kappel
Centro de Ciências Computacionais
Universidade Federal do Rio Grande
Rio Grande, Brazil
0000-0002-9124-8540

Paulo L. J. Drews-Jr
Centro de Ciências Computacionais
Universidade Federal do Rio Grande
Rio Grande, Brazil
0000-0002-7519-0502

Rodrigo S. Guerra
Centro de Ciências Computacionais
Universidade Federal do Rio Grande
Rio Grande, Brazil
0000-0003-4011-0901

***Abstract*—This work aims to develop an open-source anthropomorphic hand prosthesis. The methodology involves designing a manipulator that replicates the precision grips of the human hand. The development process integrated CAD modeling and 3D printing for prototyping a biomimetic structure that combines a reinterpretation of organic anatomy with practical functionalities in a synthetic design. The prosthesis features 22 degrees of freedom, actuated by N20 motors controlled through shift registers and motor drivers, with joint position feedback provided by resistive sensors. The embedded firmware running on an ESP32 microcontroller utilizes an on-off control strategy with a dead zone to achieve accurate joint positioning. Experimental tests demonstrate the system's ability to perform various grasp types and manipulate small objects, highlighting its potential applications in assistive robotics and dexterous manipulation.**

***Index Terms*—Prosthesis, Biomimetics, Prototype, 3D printing, Robotic hand**

I. Introduction

According to the SIHSUS database, between 2008 and 2015, a total of 361,585 hospital amputations of upper and lower limbs were recorded just in Brazil [1]. This data highlights the relevance of progress in neuroscience, engineering, and medicine, as well as the importance of advancing prosthetic technologies that enable the development of increasingly capable artificial limbs [2]. Given the existence of different levels of amputations, a prosthesis can vary significantly in complexity and focus, ranging from purely aesthetic components to sophisticated robotic and sensory systems.

In the context of upper-limb prostheses, one of the greatest challenges lies in replicating the dexterity and versatility of the human hand. The hand is an extremely complex biomechanical system, composed of 27 bones interconnected by multiple joints and actuated by a combination of muscles and tendons, which enable a wide range of movements, including fine motor skills, grasping, and manipulation [3], [4]. This complexity poses significant challenges in the development of anthropomorphic robotic hands that aim to reproduce both the mechanical structure and the functional behavior of a natural hand.

Several projects and initiatives have been dedicated to developing robotic hands and prosthetic systems with varying degrees of anthropomorphism and control complexity. Despite significant advances in the field, the high cost, complexity, and maintenance requirements of these devices still represent barriers to large-scale adoption, particularly in developing countries. Therefore, there remains a demand for solutions that are both technically effective and accessible in terms of manufacturing and cost.

In this context, the present work proposes the development of an anthropomorphic robotic manipulator with 22 degrees of freedom, designed to mimic the kinematic behavior of the human hand. The work was developed based on an in-depth study of hand osteology and biomechanics, resulting in a structure that functionally represents each bone and joint. The prototype was entirely developed using 3D-printed components and low-cost electronic elements.

This paper provides a detailed description of the development process, covering aspects of mechanical design, actuation system, control firmware, and the electrical architecture of the manipulator. Additionally, the results obtained from functional tests are presented, demonstrating the system's ability to perform various poses and grasp objects. These results highlight the applicability of the proposed system in both the development of robotic manipulators and assistive robotics solutions.

The work is divided as follows: Section II discusses related work; Section III analyzes the anatomy of a human hand; Section IV discusses the developed robotic hand; Section V shows results; and Finally, Section VI draws conclusions.

*This study was partly supported by the National Council for Scientific and Technological Development (CNPq).

II. Related Work

Over the past 40 years [7], there have been significant advances in the development of dexterous hands, which are devices designed to partially or fully replicate the dexterity of the human hand [8] [9]. Dexterous hands can be classified as pneumatic or electric. Pneumatic systems, which are simpler, were used in early manipulators and are still present in some modern models. On the other hand, electric systems, utilizing DC motors, have enabled the creation of more compact and precise prostheses with proportions closer to those of the human hand. This approach is adopted in this work [10] [2].

The ILDA (Integrated Linkage-Driven Dexterous Anthropomorphic) robotic hand [5] was designed based on a linkage-driven actuation mechanism, aiming to optimize kinematic performance. The main structure consists of five anthropomorphic fingers, each engineered to replicate the natural movements of human joints. The fingers feature three main joints, enabling each finger to perform flexion, extension, abduction, and adduction movements with high precision. This design enables precise control over grasping and manipulation tasks.

A modular architecture is a key aspect of the ILDA hand design. All five fingers share a common base structure, with variations in length only for the thumb and the little finger. The fingers are attached to a carpal-like structure, enabling the metacarpals to be assembled in a fully modular fashion.

The electronic system features force/torque (F/T) sensors embedded at the fingertips, which are connected to dedicated control boards. The choice of materials varies according to structural requirements: high-strength components such as the finger frames, proximal phalanges, and linkages are made of SUS303 stainless steel, while the remaining parts are constructed from 6061 aluminum. To enhance friction at the fingertips, a silicone material (KE-1300, Shin-Etsu) is applied. The actuators consist of compact DC motors (DCX 8 M, Maxon) equipped with 16:1 gearboxes and magnetic encoders (ENX 8 Mag, Maxon).

The main difference between the ILDA hand and the one developed in this work lies in the materials and structural complexity. While the ILDA uses steel and aluminum, resulting in a more robust but heavier structure, the hand developed in this work is primarily manufactured using 3D-printed polymers, making it lighter. Furthermore, the ILDA features a more complex transmission system, especially in the fingers, which contributes to its weight of over 1 Kg, in contrast to the 500 g of the manipulator described here, making it more suitable for integration with robotic arms with lower payload capacities.

Another example is Open Bionics, a company dedicated to developing upper-limb assistive devices with the aim of making them accessible, functional, and highly customizable. By employing 3D printing technologies in the manufacturing process, the company achieves reductions in both production costs and lead time [6]. This strategy enables the devices to be precisely adapted to meet the specific needs of each user.

The bionic hand adopts an underactuated design, in which each of the five fingers is controlled by a single actuator positioned within the palm. Its transmission system relies on tendon-driven mechanisms routed through guiding tubes. Each finger comprises three phalanges, offering three rotational degrees of freedom (DoF) for flexion and extension. The thumb differs slightly, consisting of two phalanges with two DoF for flexion/extension and an additional DoF for abduction/adduction. The joints utilize elastomer-based materials, providing lightweight and durable articulation. Passive extension is facilitated by the inherent elasticity of these joints, while flexion is actuated via Dyneema cables guided through low-friction tubes. To enhance grasp stability and tactile interaction, the fingertips are covered with materials such as deformable foam, rubber tape, and anti-slip coatings.

Another example of a prosthetic system is the one developed by Will Cogley . Inspired by the anatomical structure of the human hand, the design uses servo motors mounted in the forearm to drive the joints via inextensible cables. The fingers of the bionic hand incorporate a flexible core made of materials such as nylon or springs, which allows them to return to a neutral position when the cable tension is released. To control finger movements, the system employs 21 servo motors (MG90S Tower Pro and MG996R) located in the forearm, excluding two additional motors dedicated to the wrist mechanism [11].

In the latest versions of the manipulator, potentiometers have been added to the joints, enabling real-time feedback of each joint's position. This enhancement allows for significantly more precise control over the manipulator's movements.

The main differences between Will's manipulator and the one developed in this work are the type and number of motors used, as well as the finger extension mechanism. A significant issue is that any external force in the flexion direction can move the finger, as the spring does not provide enough resistance. Increasing the spring force would make it too difficult for the motor to move the finger.

III. Anatomy

Analyzing the osteology of the human hand, as shown in Fig. 1, it consists of 27 bones, organized into three groups: the carpal bones (wrist), metacarpal bones (palm), and phalanges (fingers) [3]. The hand consists of eight carpal bones and five metacarpal bones, which are connected through the carpometacarpal (CMC) joints, resulting in a total of five articulations. Each metacarpal is associated with a specific finger: the first metacarpal connects to the thumb, the second to the index finger, the third to the middle finger, the fourth to the ring finger, and the fifth metacarpal corresponds to the little finger.

The thumb is composed of the proximal and the distal phalanges. The base of the proximal phalanx connects to the metacarpal, forming the metacarpophalangeal (MCP) joint. The base of the distal phalanx articulates with the head of the

https://openbionics.com/

https://willcogley.portfoliobox.net/

proximal phalanx, forming the interphalangeal (IP) joint [4]. The remaining fingers are composed of three phalanges: proximal, middle, and distal. Similar to the thumb, the base of each proximal phalanx connects to the corresponding metacarpal, forming the MCP joint. The head of the proximal phalanx articulates with the base of the middle phalanx, forming the proximal interphalangeal (PIP) joint. Finally, the base of the distal phalanx articulates with the head of the middle phalanx, forming the distal interphalangeal (DIP) joint.

For the characteristic movement of the last two joints of each finger, a flexor muscle originating from the humerus (the upper arm bone) inserts into the base of the middle phalanges of the second to fifth fingers, enabling flexion of the proximal interphalangeal (PIP) joints. Flexion of the distal interphalangeal (DIP) joints is driven by a flexor muscle that originates from the ulna (the forearm bone) and inserts into the base of the distal phalanges of the same fingers. Extension of the middle and distal phalanges is achieved by a common extensor inserted into the dorsal region of the distal phalanx base [4]. This anatomical configuration allows the human finger to perform coupled flexion of the two distal joints.

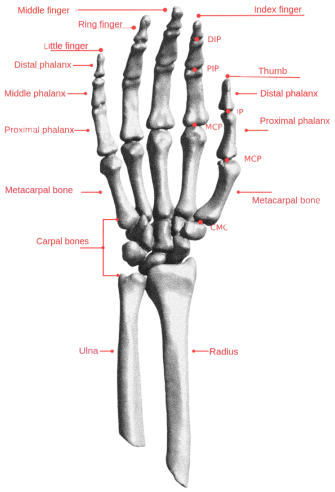

Fig. 1. Anatomical Structure of the Human Hand.

IV. Mechanical Structure

The open-source anthropomorphic prosthesis developed in this work was designed with 28 segments printed on an Ender 3D V2 printer , aiming to replicate the function of each bone. The carpal structure was simplified, with the eight carpal bones condensed into four distinct segments. These include a rigid component that connects the metacarpals, maintaining only one functional carpometacarpal (CMC) joint—specifically, the thumb's CMC—while the other three joints were fixed. Additionally, three other components were introduced: two represent the wrist's rotational joints, and a third connects the thumb's metacarpal to the carpus.

In the prosthesis, the thumb consists of two segments that represent the proximal and distal phalanges. The base of the proximal phalanx connects to the metacarpal, forming a joint analogous to the human metacarpophalangeal (MCP) joint. The distal phalanx connects to the head of the proximal phalanx, forming a joint equivalent to the human interphalangeal (IP) joint.

Regarding the other fingers, there is a slight distinction between the biological hand and the artificial prosthesis. In the prosthesis, the three bones present in each human finger are represented by four distinct segments. Three of these correspond to the proximal, middle, and distal phalanges, while the fourth segment connects the metacarpal to the proximal phalanx. This additional segment simulates a specific function of the MCP joint, which, in addition to allowing flexion along the X-axis (pitch), also enables movement along the Y-axis (roll), similar to a fan-opening motion. This movement is referred to as abduction when the fingers move apart and adduction when they move closer together. This additional segment is also present in the thumb, connecting the carpus to the metacarpal, thereby providing a greater range of motion. Fig. 2 illustrates a diagram comparing the skeletal structure of the human hand with the prosthesis designed in this work.

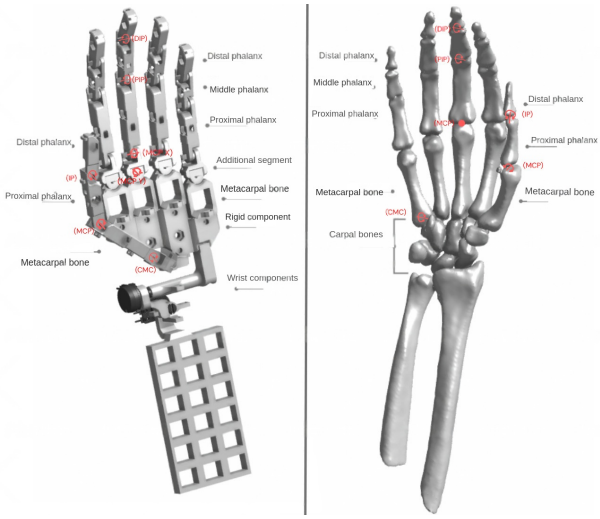

Fig. 2. Structural Mirroring Between the Artificial Limb and the Human Limb.

A more detailed analysis of the finger structure in the artificial limb developed in this work reveals certain adaptations compared to the human hand. The phalanges, as well as the entire prosthesis, are fully modeled using CAD (Computer-Aided Design) tools on the Onshape platform and prototyped through 3D printing. The phalanges are connected to each other via a bearing located at the head of each phalanx, which is attached to a nut at the base of the subsequent phalanx using a screw. This assembly forms a revolute joint that enables finger flexion and extension. Between the proximal phalanx and the metacarpal, an additional segment is incorporated to allow adduction and abduction movements. To capture the joint positions, a potentiometer is integrated into each joint,

https://www.creality.com/br/products/ender-3-v2-neo-3d-printer.

https://www.onshape.com/.

enabling real-time reading of the angular position of each finger segment. Fig. 3 shows a detailed diagram of all the elements that compose the finger structure.

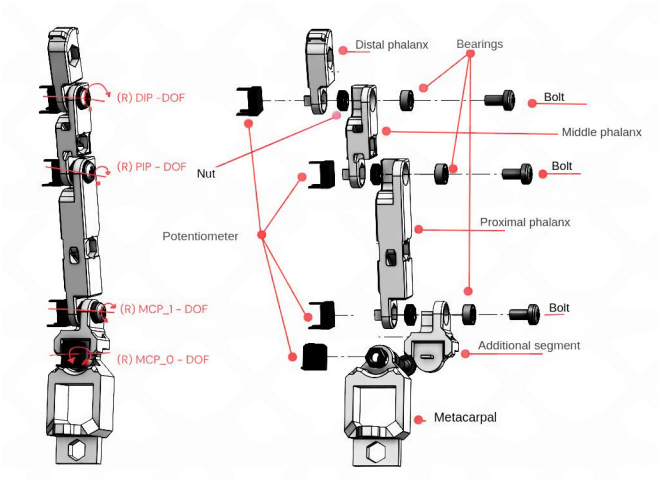

Fig. 3. Diagram of the Finger Structure. On the left, the fully assembled finger is shown, while on the right, an exploded view of the structure is presented, along with a detailed description of each component illustrated in the figure.

In the prosthesis, a nylon cable is attached to the top of the frontal side of the segment corresponding to the distal phalanx of the human hand. When tensioned by an actuator, this cable produces the flexion movement of the finger's two distal joints. For the extension movement, another nylon cable is attached to the top of the dorsal side of the distal phalanx segment. When this cable is tensioned by the actuator, it generates the extension of the same two joints. The same actuator is responsible for both flexion and extension, with the direction of rotation determining which movement is performed.

However, this configuration resulted in discontinuous movement of the finger's two distal joints, with the proximal interphalangeal (PIP) joint flexing first, followed by the distal interphalangeal (DIP) joint. To achieve coordinated motion between the joints, a cable was added, attached at the front top of the distal phalanx, routed through the middle phalanx, and fixed to the front of the proximal phalanx. Another cable was also inserted at the front top of the distal phalanx, passing through the middle phalanx and anchored to the front of the proximal phalanx. The incorporation of these two cables enabled the finger to perform movements similar to those of the human hand.

Finally, the function of muscles and tendons in the human hand is replicated by actuators and nylon cables. The prosthesis incorporates a total of 17 DC motors that act as the hand's muscles, each responsible for the flexion and extension of at least one joint of the device. These motors are located at the base of the prosthesis, corresponding to the forearm in the human limb. Motor movements are transmitted to the phalanges via two nylon cables, with one end of each attached to the actuator and the other fixed to the front or dorsal side of each phalanx. The prosthesis features a total of 22 joints, with four joints per finger and two joints for the wrist.

A. *Hardware*

The prosthesis requires 17 motors to perform the essential movements needed for executing different types of grips. The actuator selected for the system's development is the DC Mini Metal Gear Motor, commonly known as the N20 motor. This is a direct current (DC) motor widely used in robotics applications. Its gearbox, composed of metal gears, provides high torque and low revolutions per minute (RPM), operating within a voltage range of 3 to 12 V.

For motor control, the L293D Dual H-Bridge Motor Driver integrated circuit (IC) was used. This enables simultaneous control of two DC motors, allowing for both speed variation and reversal of the motor shaft rotation direction. The L293D supports bidirectional currents of up to 600 milliamperes and operating voltages ranging from 4.5 to 36 V.

Another key component in the manipulator's electronic system is the 74HC595 integrated circuit. This is an 8-bit shift register with a 3-state latch output, used to expand the digital outputs of a microcontroller. It operates within a voltage range of 2 to 6 V and supports an output current of up to 30 mA. By using this IC, it is possible to extend three digital outputs from the controller into n outputs, enabling the development of more complex projects.

Developed by Espressif Systems, the ESP32 is a microcontroller commonly used in IoT (Internet of Things) applications due to its extensive range of integrated features, including Wi-Fi and Bluetooth. The module is equipped with a dual-core processor running at up to 240 MHz, 520 KBytes of RAM, and 4 MB of Flash memory.

The ESP32 provides 34 GPIO (General Purpose Input/Output) pins, all of which can be configured for PWM (Pulse-Width Modulation). In theory, up to 16 PWM channels can be used simultaneously via hardware. The microcontroller also includes 18 ADC (Analog-to-Digital Converter) pins and 2 DAC (Digital-to-Analog Converter) pins, making it a highly versatile choice for a wide variety of projects.

The potentiometer is a key component for the joint position feedback system in the manipulator. Given the anthropomorphic characteristics of the design, a compact potentiometer was required to be integrated into the manipulator's joints. For this purpose, the RM065 model was selected, with dimensions of $7\,\text{mm} \times 6.4\,\text{mm} \times 5\,\text{mm}$.

Each finger includes four potentiometers: one mounted on the metacarpal (MCP_0 joint), one on the additional segment (MCP_1 joint), and two on the proximal phalanx (PIP joint) and middle phalanx (DIP joint). The wiper of each potentiometer is mechanically coupled to the subsequent segment of the finger, providing real-time feedback on the angular position.

The manipulator comprises a total of 22 potentiometers distributed across its joints. Due to the large number of

https://www.ti.com/lit/ds/symlink/l293.pdf.
https://www.ti.com/lit/ds/symlink/l293.pdf.
https://www.diodes.com/assets/Datasheets/74HC595.pdf.
https://www.espressif.com/sites/default/files/documentation/esp32-c3_datasheet_en.pdf
https://www.bochen-cn.com/rm065.html

sensors, two 16-channel analog multiplexers are employed to enable the acquisition of all signals. The multiplexer is an electronic component capable of routing up to 16 analog or digital inputs to a single output, allowing efficient and scalable signal management for the entire system.

Fig. 4 presents a detailed diagram of the circuit organization designed to read all the potentiometers in the system. The diagram clearly illustrates the connection from the sensor reading pins to the multiplexer, and from the multiplexer to the control module. For simplicity, the power supply connections for the potentiometers have been omitted from the diagram. They are powered by the 3V output from the ESP32.

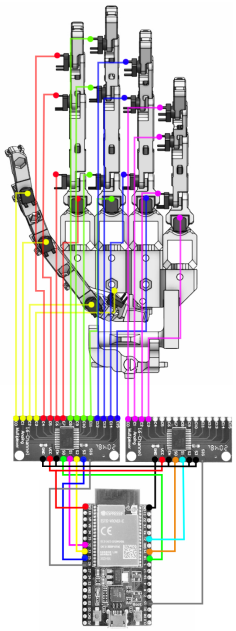

Fig. 4. The diagram shows the resistive sensor connections in the manipulator. At the top, each color represents a specific finger (yellow = thumb, red = index, blue = middle, pink = little). At the bottom, the connections between the ESP32 module and the multiplexers are shown, but the colors here do not follow the top section's scheme.

The actuation system for the N20 motors uses eight L293D driver circuits. Since the control does not require PWM, the operation of the L293D is straightforward: setting input 1 to logic high (3 V from the ESP32) and input 2 to logic low (0 V from the ESP32) causes the motor to rotate counterclockwise. To rotate clockwise, the values are inverted. The L293D drivers are powered by a 5V, 5A power supply, which is sufficient to handle the simultaneous operation of up to 15 motors.

The 74HC595 shift register is responsible for sending the appropriate logic signals to the L293D drivers, activating each motor at the correct time. The system operates by transmitting a set of 32 bits from the ESP32 to the ICs, which receive the data serially via the data input (DS) pin. These bits are shifted into the internal register with each clock pulse (SCKL). Once the data transfer is complete, a latch signal (RCLK) transfers the values to the parallel outputs, which then control the motors synchronously. Fig. 5 shows a complete diagram of the circuit responsible for driving and controlling the manipulator's motors.

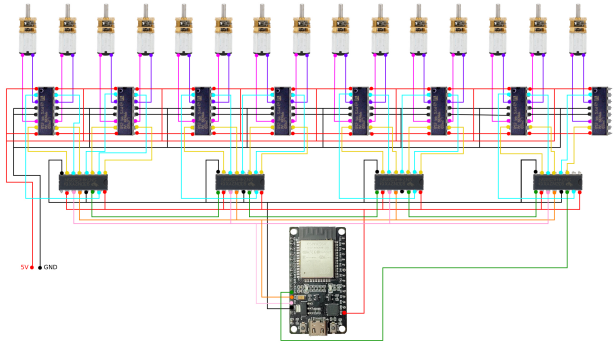

Fig. 5. Diagram of the manipulator's electrical and digital circuit. The figure is divided into four levels: the first level contains the ESP32 and the motor power supply; the second level shows the 74HC595 shift registers; the third level presents the L293D motor drivers; and the final level includes the motors.

B. Firmware

The manipulator's firmware is written in C/C++ using the Arduino IDE platform and is responsible for controlling the prosthetic device's basic functions. Its main task is to read and process the information detected by the potentiometers, using this data to control the joints through actuator activation. The actuators' rotation moves the manipulator's joints as required.

Although the ESP32 has 16 PWM channels, it is not possible to configure them all with different frequencies due to its having only four timers. This means that some outputs will always share the same PWM frequency, which complicates the implementation of proportional or PID control.

Due to the inability to use PWM on all channels, a constant actuator speed was defined. For motor actuation, an On-Off control with a dead zone was used, which, combined with the 74HC595 shift registers, enabled efficient activation of the manipulator's motors using only three microcontroller outputs.

Actuator control is performed through logic that manages motor movement based on the error between the current motor position and the target value received via serial input. This approach ensures precise motor control, aligning movements with the desired positions.

The control logic operates with three parameters: the motor index to be controlled, its current position (read via the multiplexer values), and the target position. Based on these, the control logic follows three main steps. First, the error is calculated as the difference between the target position and the current motor position. This value is used to determine the direction and magnitude of the required adjustment.

In the directional adjustment step, if the error exceeds a positive threshold, the motor is activated in one direction to approach the target position. If the error is less than a negative threshold, the motor is activated in the opposite direction. If the error lies within an acceptable range (dead zone), the motor is turned off. Fig. 6 shows a diagram illustrating the functioning of the threshold and dead zone.

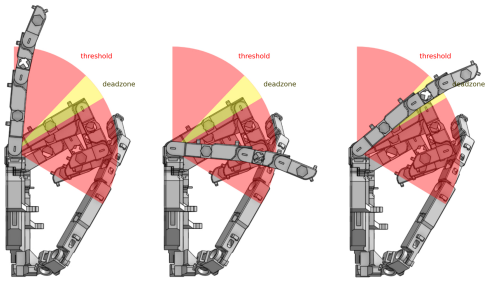

Fig. 6. The figure illustrates the directional adjustment according to the error.

V. Results

When rotating the horns on the motor shafts, all joints of the prosthesis exhibited flexion and extension movements as expected. The electrical actuation of the motors accurately replicated this behavior, demonstrating that the mechanical and electrical systems designed are capable of performing the intended movements. One issue identified in the system is that the cables occasionally unwind from the horns and become tangled, potentially causing joint blockage. Aside from this issue, the system functions exactly as intended.

When sending sets of values to the joints, the firmware correctly interpreted the commands and activated the motors to position the joints at the desired states based on the readings from the potentiometers. This behavior was consistently reproduced for different poses, including actions such as grasping objects and performing specific gestures.

In the videos presented, different tests performed with the manipulator can be observed. In the first video, the joint control of the manipulator is demonstrated through a graphical interface using ROS 2 [12]. In the second video , a programmed sequence shows the manipulator performing pinch movements with all fingers. The third video displays the manipulator holding a small object, highlighting its ability to execute precision movements.

These results demonstrate that the overall system, comprising mechanical, electrical, and control components, operates as expected. The prosthesis was able to achieve various poses and successfully grasp some objects, as illustrated in Fig. 7, which showcase real applications of the actual developed prosthesis.

VI. Conclusions

This work developed an open-source anthropomorphic manipulator with 22 joints, detailing the operation of each component of the robotic hand structure, and presenting similarities with the human hand. The materials used for its prototyping were also described, including the actuators, integrated circuits (ICs), sensors, and the microcontroller employed in its development. The results demonstrated that the prosthetic structure is capable of performing a wide variety of poses with autonomy and precision, being able to grasp several objects.

Control test video: https://youtu.be/WiAowT8e864
Pinch movement video: https://youtube.com/shorts/rBn_vVieEvY
Grasping an object video: https://youtube.com/shorts/heSxoNY5Cx4

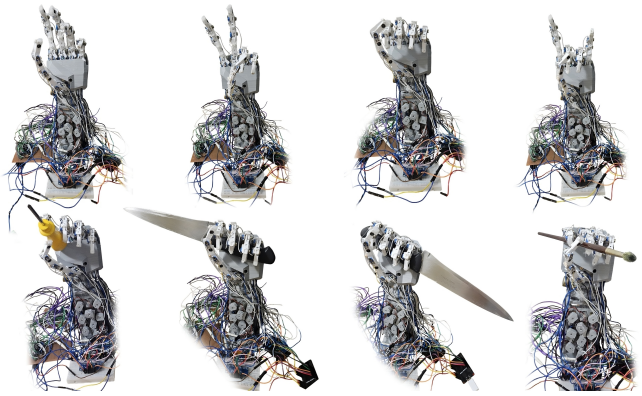

Fig. 7. This figure presents real images of the fully assembled manipulator performing different types of poses and grasps. In the upper section, the hand performs free poses, while in the lower section, it manipulates objects such as a knife, a brush, and a Phillips screwdriver.

For future versions of the manipulator, the structural components of the robotic hand are expected to be manufactured using resin-based 3D printing, which would allow for the creation of more complex, precise, and robust parts. Another planned improvement is the development of a printed circuit board (PCB), which would drastically enhance the quality and reliability of the manipulator's electrical system.

References

[1] A. M. Peixoto, S. A. Zimpel, A. C. A. Oliveira, R. L. S. Monteiro, and T. K. G. Carneiro, "Prevalência de amputações de membros superiores e inferiores no estado de Alagoas atendidos pelo SUS entre 2008 e 2015," *SciELO Brazil*, 2017.

[2] M. Niedernhuber, D. G. Barone, and B. Lenggenhager, "Prostheses as extensions of the body: Progress and challenges," *Neuroscience & Biobehavioral Reviews*, vol. 92, pp. 1–6, 2018.

[3] A. Tang and M. Varacallo, "Anatomy, Shoulder and Upper Limb, Hand Carpal Bones," *StatPearls [Internet]*, 2022.

[4] D. G. Arias, A. C. Black, and M. Varacallo, "Anatomy, Shoulder and Upper Limb, Hand Bones," *StatPearls [Internet]*, 2023.

[5] U. Kim, D. Jung, H. Jeong, J. Park, H.-M. Jung, J. Cheong, H. R. Choi, H. Do, and C. Park, "Integrated linkage-driven dexterous anthropomorphic robotic hand," *Nature Communications*, 2021.

[6] G. P. Kontoudis, M. V. Liarokapis, A. G. Zisimatos, C. I. Mavrogiannis, G. P. Kontoudis, and K. J. Kyriakopoulos, "How to Create Affordable, Anthropomorphic, Personalized, Light-Weight Prosthetic Hands," Control Systems Lab, School of Mechanical Engineering, National Technical University of Athens, Tech. Rep., Oct. 2015.

[7] Y. Li, P. Wang, R. Li, M. Tao, Z. Liu, and H. Qiao, "A Survey of Multifingered Robotic Manipulation: Biological Results, Structural Evolvements, and Learning Methods," *Frontiers in Neurorobotics*, 2022

[8] M. Andrychowicz, B. Baker, M. Chociej, R. Józefowicz, B. McGrew, J. Pachocki, A. Petron, M. Plappert, G. Powell, A. Ray, J. Schneider, S. Sidor, J. Tobin, P. Welinder, L. Weng, and W. Zaremba, "Learning dexterous in-hand manipulation," *The International Journal of Robotics Research*, vol. 39, no. 1, pp. 3–20, 2020. doi: 10.1177/0278364919887447.

[9] F. Veiga, R. Akrour, and J. Peters, "Hierarchical Tactile-Based Control Decomposition of Dexterous In-Hand Manipulation Tasks," *Frontiers in Robotics and AI*, vol. 7, 2020. doi: 10.3389/frobt.2020.521448.

[10] J. D. Hubbard, R. Acevedo, K. M. Edwards, A. T. Alsharhan, Z. Wen, J. Landry, K. Wang, S. Schaffer, and R. D. Sochol, "Fully 3D-printed soft robots with integrated fluidic circuitry," *Science Advances*, 2021.

[11] W. Cogley, "Biomimetic Mechatronic Hand 2018 Report," Technical Report, 2018.

[12] M. Quigley, K. Conley, B. Gerkey, J. Faust, T. Foote, J. Leibs, R. Wheeler, A. Y. Ng, "ROS: an open-source Robot Operating System," *ICRA Workshop on Open Source Software*, 2009.